

The Probabilistic Stability of Stochastic Gradient Descent

Liu Ziyin¹, Botao Li², Tomer Galanti³, Masahito Ueda^{1,4}

¹*Department of Physics, The University of Tokyo, 7-3-1 Hongo, Bunkyo-ku, Tokyo 113-0033, Japan*

²*Laboratoire de Physique de l'Ecole normale supérieure, ENS, Université PSL,
CNRS, Sorbonne Université, Université de Paris Cité, Paris, France*

³*Center of Brains, Minds and Machines (CBMM), Massachusetts Institute of Technology, Cambridge, MA, USA*

⁴*RIKEN Center for Emergent Matter Science (CEMS), Wako, Saitama 351-0198, Japan*

March 24, 2023

Abstract

A fundamental open problem in deep learning theory is how to define and understand the stability of stochastic gradient descent (SGD) close to a fixed point. Conventional literature relies on the convergence of statistical moments, esp., the variance, of the parameters to quantify the stability. We revisit the definition of stability for SGD and use the *convergence in probability* condition to define the *probabilistic stability* of SGD. The proposed stability directly answers a fundamental question in deep learning theory: how SGD selects a meaningful solution for a neural network from an enormous number of solutions that may overfit badly. To achieve this, we show that only under the lens of probabilistic stability does SGD exhibit rich and practically relevant phases of learning, such as the phases of the complete loss of stability, incorrect learning, convergence to low-rank saddles, and correct learning. When applied to a neural network, these phase diagrams imply that SGD prefers low-rank saddles when the underlying gradient is noisy, thereby improving the learning performance. This result is in sharp contrast to the conventional wisdom that SGD prefers flatter minima to sharp ones, which we find insufficient to explain the experimental data. We also prove that the probabilistic stability of SGD can be quantified by the Lyapunov exponents of the SGD dynamics, which can easily be measured in practice. Our work potentially opens a new venue for addressing the fundamental question of how the learning algorithm affects the learning outcome in deep learning.

1 Introduction

Stochastic gradient descent (SGD) is the main workhorse for optimizing deep learning models. A fundamental problem in deep learning theory is to characterize how SGD selects the solution of a deep learning model, which often exhibits remarkable generalization capability. At the heart of this problem is the *stability* of SGD because the models trained with SGD stay close to the solution where the dynamics is stable and moves away from unstable solutions. Solving this problem thus hinges on having a good definition of the stability of SGD. The established literature often defines the stability of SGD as a function of the variance of the model's parameters or gradients during training. The hidden assumption behind the mainstream thought is that if the variance diverges, then the training becomes unstable (Wu et al., 2018; Zhu et al., 2018; Liu et al., 2020, 2021; Ziyin et al., 2022b). In some sense, the thought that the variance of the parameters matters the most is also an underlying assumption of the deep learning optimization literature, where the utmost important quantity is how fast the variance and the expected distance of the parameters decay to zero (Vaswani et al., 2019; Gower et al., 2019). We revisit this perspective and show that a variance-based notion of stability is insufficient to understand the empirically observed stability of training of SGD. For example, we demonstrate natural learning settings where the variance of SGD diverges, yet the model still converges with high probability.

In this work, we study the *convergence in probability* condition to understand the stability of SGD. We then show that this stability condition can be quantified with a stochastic extension of the Lyapunov

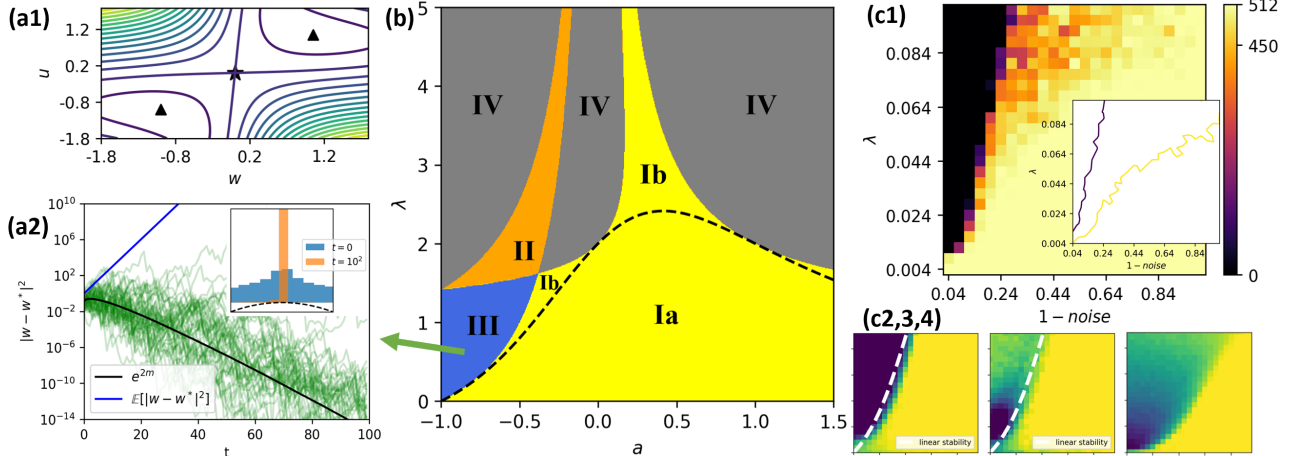


Figure 1: **SGD exhibits a complex phase diagram through the lens of probabilistic stability.** (a1) Landscape of a simple two-layer tanh neural network: $f(x) = u \tanh(wx)$. Triangles show the location of the global minima. The star shows the origin, which is a saddle point. (a2) With a large learning rate, SGD converges to the saddle in probability, even though it escapes in expectation. Here, m is the Lyapunov exponent times t , which agrees well with a typical learning trajectory. The inset shows the distribution of the parameters before and after training. (b) A phase diagram of SGD. For a matrix factorization saddle point, the dynamics of SGD can be categorized into at least five different phases. Phase **I**, **II**, and **IV** correspond to a successful escape from the saddle. Phase **III** is the case where the model converges to a low-rank saddle point. Phase **I** corresponds to the case $w_t \rightarrow_p u_t$, which signals correct learning. In phase **Ib**, the model also converges in variance. Phase **II** corresponds to stable but incorrect learning, where $w_t \rightarrow_p -u_t$. Phase **IV** corresponds to complete instability. See Section 4.2 for a detailed discussion. (c1) Numerical results on training with ResNet18 for an image classification task. The color shows the penultimate-layer representation of Resnet18 trained with different levels of label noise. The inset shows the estimated boundary of rank 511 and 1. We observe that the phase boundary agrees qualitatively with simple two-layer networks without nonlinearity (c2) and with the tanh activation (c3), for which phase boundaries can be theoretically computed. (c4) The phase diagram is not limited to SGD but also applies to models trained with Adam, suggesting a universal effect that may be attributable to all first-order learning algorithms with minibatch sampling.

exponent (Lyapunov, 1992), a quantity rooted in the study of dynamical systems and has been well understood in physics and control theory (Eckmann and Ruelle, 1985).

The main contribution of this work is to propose a new notion of stability that sheds light on how SGD selects solutions and multiple deep-learning phenomena that can only be understood by this notion. Perhaps the most important implication of our theory is the characterization of the highly nontrivial and practically important phase diagram of SGD in a neural-network loss landscape (as illustrated in Figure 1).

2 Problem Setting

In this section, we introduce the problem setting, describe the standard linear stability theory, and discuss its implications for understanding the stability of minibatch SGD.

Definitions. In a standard supervised learning setting, we are given a data distribution $p(x, y)$ from which independently sampled input-label pairs (x, y) are drawn. For notational concision, we let $y = y(x)$ be a function of x , so that $p(x, y) = p(x)$. We allow $p(x)$ to be a uniform distribution over samples from a given dataset of size N or a distribution over a continuous space. The training loss is defined as the empirical expectation $L(w) = \mathbb{E}_x[\ell(w, x)]$ of a sample-wise loss function $\ell(w, x)$, where w is the vectorized model parameters.

Model training proceeds with the stochastic gradient descent (SGD) algorithm with a batch size S and learning rate λ . At each iteration t , SGD computes the gradient by using a randomly drawn mini-batch of

S samples $(x_j)_{j=1}^S$ from $p(x)$. Then, SGD updates the parameters w according to the following rule:

$$w_{t+1} = w_t - \frac{\lambda}{S} \sum_{j=1}^S \nabla_w \ell(w_t, x_j). \quad (1)$$

In this definition, we can handily define gradient descent (GD) as the infinite S limit of SGD. To study the stability of SGD, we will focus on the notion of convergence in probability, denoted by \rightarrow_p . The weight parameters w_t is said to converge to c in probability if for any $\epsilon > 0$ $\lim_{t \rightarrow \infty} \mathbb{P}(|w_t - c| > \epsilon) = 0$.

A choice of the learning rate λ and that of the batch size constitutes an important practical problem that involves complicated tradeoffs. On the one hand, one wants to use a large learning rate and a small batch size so that the model trains faster and generalizes better (Shirish Keskar et al., 2016; Hoffer et al., 2017; He et al., 2019; Li et al., 2019; Galanti and Poggio, 2022). On the other hand, one wants to use a small learning rate and a large batch size to keep the training stable and convergent. At the core of this tradeoff thus lies the notion of stability. To understand the stability of an interpolation minimum, we follow the standard practice and consider the linearized dynamics of SGD around a local minimum w^* :

$$w_{t+1} - w^* = w_t - \frac{\lambda}{S} \sum_{j=1}^S \hat{H}(w^*, x_j)(w_t - w^*), \quad (2)$$

where $\hat{H}(w, x) := \nabla_w^2 \ell(w, x)$ is the sample-wise Hessian.

The previous literature focuses on variants of the following notion of stability. GD is said to be stable at w^* if $w_t - w^*$ converges to zero. For SGD, the learning is considered stable if $\mathbb{E}[\|w_t - w^*\|^2] \rightarrow 0$. In probability theory, this condition is equivalent to the condition that w_t converges w^* in mean square. It is elementary to show that convergence in mean square implies the convergence in probability but not vice versa. We will show that these two convergence conditions are dramatically different for SGD and that convergence in mean square is too strong a condition to understand the actual learning behavior of SGD in deep learning.

Stability of a minimal model. To investigate the stability of the SGD algorithm, we examine a simple one-dimensional linear regression problem. The training loss function for this problem is defined as $L(w) = \frac{1}{N} \sum_i^N (wx_i - y_i)^2$.

For GD, the dynamics diverge when the learning rate is larger than twice the inverse of the largest eigenvalue of the Hessian. To see this, let $H = \mathbb{E}_x[\hat{H}(w^*, x)]$ denote the Hessian of L and h its largest eigenvalue. The dynamics of GD leads to $\|w_{t+1}\| = \|w_0(I - \lambda H)^t\| \propto |1 - \lambda h|^t$. Divergence happens if and only if $|1 - \lambda h| > 1$. The range of viable learning rates is thus given by:

$$\lambda_{\text{GD}} \leq 2/h = 2/\mathbb{E}_x[x^2]. \quad (3)$$

Naively, one would expect that a similar condition approximates the stability condition for the case when mini-batch sampling is used to estimate the gradient. This has indeed been argued to be the case in the recent works (Wu et al., 2018; Liu et al., 2021; Ziyin et al., 2022b).

For SGD, the stability condition is the same as the condition that the second moment of SGD decreases after every time step, starting from an arbitrary initialization (see Appendix A):

$$\lambda_{\text{DS}} \leq \frac{2S^2 \mathbb{E}[x^2]}{\mathbb{E}[x^4] + (S-1)^2 \mathbb{E}[x^2]^2}. \quad (4)$$

Also related is the stability condition proposed by Ziyin et al. (2022b), who showed that starting from a stationary distribution, w stays stationary under the condition $\lambda_{\text{SS}} < \frac{2}{h} \frac{1}{1+1/S}$, which we call the stationary linear stability condition (SS). Namely, when minibatch sampling is used, one expects the dynamics to be less stable by a factor of $1 + 1/S$. When we have batch size 1, the stability condition halves: $\lambda < 1/h$. For all stability conditions, we denote the maximum stable learning rate with an asterisk: λ^* . The most important prediction made by the linear stability theories is that SGD prefers flatter minima to sharper ones because the linear stability is lost as one increases the learning rate above $2/h$, which is believed to lead to better performance (Zhu et al., 2018; Wu et al., 2018; Xie et al., 2020; Wu et al., 2022). On the contrary, we

will show that this mechanism of minimum selection is not what probabilistic stability implies. Throughout this work, we use the term “linear stability theory” to refer to any theory of stability that is based on the statistical moments in order to emphasize their difference from probabilistic stability, which is our main proposal.

3 Convergence in Probability Condition for SGD

We now present the main theoretical results of this work. We first show that there exist critical learning rates that are far larger than $2/h$ for which SGD converges in probability to the global minimum. We then show that such learning rates are not special or isolated points but span a rather large space with a nonzero measure. Lastly, we prove the connection of the notion of convergence in probability to a stochastic generalization of the Lyapunov exponent, which could serve as a foundation of future study of the probabilistic stability in the context of deep learning.

3.1 Critical Learning Rates

We begin by demonstrating a specific case to illustrate our analysis. Let us consider a simple interpolation regime, where all data points $(x, y) \in \mathbb{R}^2$ lie on a straight line. In this situation, the loss function has a unique global minimum of $w = y_i/x_i$ for any x_i . Our initial question is: what is the maximum learning rate that can be used for SGD without causing divergence? We prove that for all i , SGD is convergent in probability if $\lambda = 1/x_i^2$. Therefore, the largest stable learning rate is roughly given by:

$$\lambda_{\max} = 1/x_{\min}^2. \quad (5)$$

However, for these special choices of learning rates, linear stability is not always guaranteed. As mentioned earlier, convergence in mean occurs when $\lambda \leq \lambda_{DS}^*$, but this condition does not hold when $\lambda = 1/x_{\min}^2$ and $x_{\min} < \mathbb{E}[x_i]/2$, which is often the case for standard datasets. This result shows that the maximal learning rate that ensures stable training can be much larger than the maximal learning rate required for convergence in mean (cf. (4)). For a fixed value of $\mathbb{E}[x^2]$, x_{\min}^2 can be arbitrarily small, which means that the maximal stable learning rate can be arbitrarily large. Another consequence of this result is that the stability of SGD depends strongly on individual data points and not just on summary statistics of the whole dataset.

3.2 Are Such Learning Rates Isolated?

The important question is whether the critical learning rates in Proposition 3 are special or not, and whether the convergence is robust against perturbations in the learning rate. The answer to both questions is yes. We show that there exists a wide neighborhood close to the critical learning rates such that the model still converges in probability. We note that convergence in probability is sufficient to ensure that SGD is stable at the corresponding learning rate for all practical purposes, as the probability of an unstable trajectory being observed decreases to zero as the number of training steps increases.

Let $v_t := w_t - y_t/x_t = w_t - w^*$. The SGD dynamics in terms of v_t can be written as

$$v_{t+1} = v_t - \lambda x_t^2 v_t. \quad (6)$$

Apparently, the unique global minimum is $v^* = 0$, i.e., $w^* = y_t/x_t$. Furthermore, because the dynamics of Eq. (6) is independent of w^* , we can assume $w^* = y_t/x_t = 0$. The following proposition gives the convergence condition.

Proposition 1. *Let λ be such that $\mathbb{E}_x[\log|1 - \lambda x^2|] \neq 0$. Then, for any w_0 , $w_t \rightarrow_p w^*$ if and only if $\mathbb{E}_x[\log|1 - \lambda x^2|] < 0$.*

It is worth remarking that this condition is distinctively different from the case when the gradient noise is a parameter-independent random vector. For example, Liu et al. (2021) showed that if the gradient noise is a parameter-independent gaussian, SGD diverges in distribution if $\lambda > 2/h$. This suggests that the fact that the noise of SGD is w -dependent is crucial for its probabilistic stability.

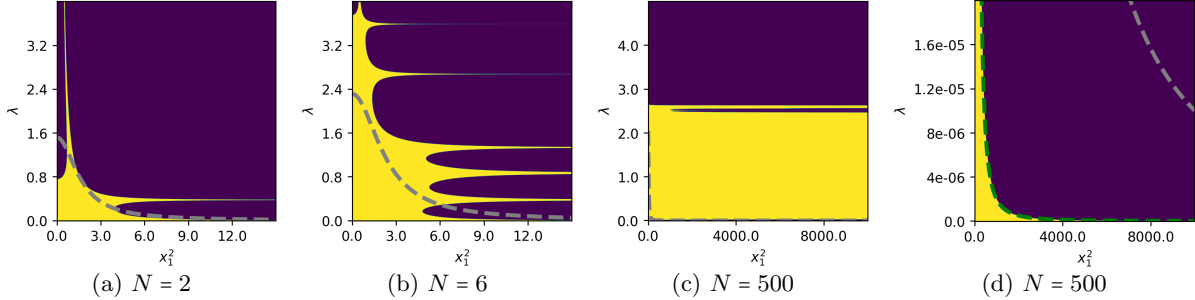


Figure 2: **Stability of SGD against a single outlier data** in a dataset of size N . Yellow denotes where SGD converges in probability, and dark blue denotes divergence. We control the norm of the first data point (x_1^2) while sampling the rest data from a standard normal distribution. (a-c) stability of SGD for different sizes of the dataset; (d) zoom-in of (c) at a small learning rate. The grey dashed curves show λ_{GD}^* , and the green dashed curve shows λ_{GD}^*/N . The intermediate finite learning rates are robust against outliers in the data, whereas the smallest learning rates are strongly sensitive to outliers in the data.

This result highlights the importance of the quantity $m := \mathbb{E}_x[\log|1 - \lambda x^2|]$ and its sign in understanding the convergence of w_t to the global minimum. When m is negative, the convergence to the global minimum occurs. If m is positive, SGD becomes unstable. We can determine when m is negative for a training set of finite size by examining the following equation:

$$m = \frac{1}{N} \sum_i \log|1 - \lambda x_i^2|, \quad (7)$$

which is negative when λ is close to $1/x_i^2$ for some $i \in 1, \dots, N$. What is the range of λ values that satisfy this condition? Suppose that λ is in the vicinity of some $1/x_i^2$: $\lambda = \delta\lambda + 1/x_i^2$, and the instability is caused by a single outlier data point $x_{\text{out}} \gg 1$. Then, m decided by the competitive contributions from the outlier, which destabilizes training, and x_i^2 , which stabilizes training, and the condition is approximately $|1 - \lambda x_i^2| < 1/|\lambda x_{\text{out}}^2|$. Because $\lambda \approx 1/x_i^2$, this condition leads to:

$$|\delta\lambda| < x_i^2/x_{\text{out}}^2. \quad (8)$$

This is a small quantity. However, if we change the learning rate to the stability region associated with another data point x_j as soon as we exit the stability region of x_i , we still maintain stability. Therefore, the global stability region depends on the density of data points near x_i . Assuming there are N data points near x_i with a variance of σ^2 , the average distance between x_i and its neighbors is approximately σ^2/N . As long as $\sigma^2/N < x_i^2/x_{\text{out}}^2$, SGD will remain stable in a large neighborhood. In practical terms, this means that when the number of data points is large, SGD is highly resilient to outliers in the data as shown in Figure 2. We see that the region of convergence in probability is very dramatic, featuring stripes of convergent regions that correspond to $1/x_i^2$ for each data point and divergent regions where $m > 0$.

Lastly, we comment that the same analysis carries over to the case of large batch size. The difference is that for $S = 1$, the distribution of the gradient only depended on the distribution of x^2 , whereas for $S > 1$, the gradient depends on a sum of squares: $\mathbb{P}(\frac{1}{S} \sum_i^S x_i^2)$. When x is Gaussian, this is a rescaled chi-squared distribution with the degree of freedom S . Let g denote the gradient on a single data. When $S \rightarrow \infty$, the distribution tends to a Gaussian with variance $v := \text{Var}[g]/S$ and mean $\mathbb{E}[g]$. In the case of infinite batch size, the dynamics becomes the same as that of GD, and the condition for convergence reduces to the prediction of the linear stability theory. When the batch size is large but not too large (namely, when the distribution is effectively a Gaussian, but its variance is not vanishingly small), the stability condition is nothing but the expectation of the quantity $\log|1 - \lambda x^2|$ against a Gaussian distribution, which exists in general and can be both negative and positive depending on its mean, variance, and λ . Also, the case when interpolation is no longer possible is more involved. Here, since there is no single parameter that fits all the batches, the location of the local minimum necessarily oscillates across batches. We analyze this case briefly in Appendix Section A.3. We now show that the above discussion carries naturally to the general linearized SGD dynamics for a multidimensional parameter space in Eq. (2).

3.3 The Stochastic Lyapunov Exponent and Probabilistic Stability

In practice, it is difficult to check the condition of convergence in probability. A remaining question is thus whether there is an easy-to-measure quantity that captures the probabilistic stability of SGD. Our theory implies that the following quantity is an important metric:

$$m_w(t) := \mathbb{E}_{w_t}[\log |w_t - w^*|^2], \tag{9}$$

where the expectation is taken over the trajectories of w_t with different samplings of the minibatch. One is interested in its time dependence and whether it is positive or negative. In fact, m/t is a stochastic generalization of the Lyapunov exponent, a quantity of fundamental importance in the study of dynamical systems. $m > 0$ corresponds to a chaotic system that loses stability at the rate m/t , and $m < 0$ corresponds to a stabilizing system that converges to a fixed point. When w^* is not accessible, one can instead study the following quantity:

$$m_L := \mathbb{E}_{w_t}[\log L(w_t)], \tag{10}$$

which expands to m_w when w_t is close to an interpolating minimum. From a dynamical system point of view, this quantity can be used to investigate the stability of stationary points of L . Alternatively, e^{m_L} can be seen as a robust estimate of the training loss, and our theory suggests that the practitioners may use this quantity as an alternative monitoring quantity to gauge the progress of training because m_L is much less sensitive to outliers due to the use of a small batch size or a large learning rate. In fact, for the example in the previous section, one can show that the condition $\mathbb{E}[\log |1 - \lambda x^2|] < 0$ is identical to the condition $m_L < 0$.

The formal connection is established in following theorem between the stochastic Lyapunov exponent and convergence in probability.

Theorem 1. *Let $g(w)$ be a function of the parameters, $\Delta g(t) := \|g(w_t) - g^*\|$, $\hat{m}_g(w_t) := \log \Delta g(w_t)$, and $m_g(t) = \mathbb{E}_w[\hat{m}_g(t)]$. Let $\text{Var}[\log \|\Delta g(t)\|] = o(t^2)$. Then, if and only if $\lim_{t \rightarrow \infty} m_g(t) < 0$, $\log \Delta g(t) \rightarrow_p 0$.*

A detailed analysis proves that the SGD dynamics in Eq. (2) indeed obeys this theorem (Section A). Note that a key assumption here is that the variance of $\log \Delta g(w_t)$ does not grow too fast, which is a mild condition that applies to SGD in general. For example, it is much weaker than the assumption that $g(t)$ has a well-controlled variance as in the linear stability theory. Generally speaking, if $g(w_t)$ follows a multiplicative process, one expects $\text{Var}[\log \|\Delta g(t)\|] \propto t$, like a Brownian motion.

4 Implications

4.1 Abnormal Sensitivity and Robustness to outliers

One important implication of our result is the robustness of SGD to outliers in comparison to gradient descent. As Figure 2 shows, the bulk region of probabilistic stability stays roughly unchanged as the outlier data point becomes larger and larger; in contrast, both λ_{GD}^* and λ_{DS}^* decreases quickly to zero. In the bulk region of the learning rates, SGD is thus probabilistically stable but not stable in the moments.

Meanwhile, in sharp contrast to this bulk robustness is the sensitivity of the smallest branch of learning rates of SGD to the outliers. Assuming that there is an outlier data point with a very large norm $c \gg N$, the largest λ_{GD} scales as $\lambda_{\max} \sim Nc^{-1}$. In contrast, for SGD, the smallest branch of probabilistically stable learning rate scales as c^{-1} , independent of the dataset size. This means that if we only consider the smallest learning rate, SGD is much less stable than GD, and one needs to use a much smaller learning rate to ensure convergence. For λ_{DS} A detailed analysis in Section A.2 shows that $\lambda_{DS}^* = (Nc)^{-1}$. Thus, the threshold of convergence in mean square is yet one order of magnitude smaller than that of probabilistic convergence. In the limit $N \rightarrow \infty$, SGD cannot converge in variance but can still converge in probability.

4.2 Phase Diagram of SGD

With this notation of stability, we can study the actual effect of mini-batch noise on a neural network-like landscape. A commonly-studied minimal model of the landscape of neural networks is a deep linear net (or deep matrix factorization) (Kawaguchi, 2016; Lu and Kawaguchi, 2017; Ziyin et al., 2022a; Wang and

Ziyin, 2022). For these problems, we understand that all local minima are identical copies of each other, and so all local minima have the same generalization capability (Kawaguchi, 2016; Ge et al., 2016). The special and interesting solutions of a deep linear net are the saddle points, which are low-rank solutions and often achieving similar training loss with dramatically different generalization performances. More importantly, these saddles points also appear in nonlinear models with similar geometric properties and they could be a rather general feature of the deep learning landscape (Brea et al., 2019). It is thus important to understand how the noise of SGD affects the stability of a low-rank saddle here. Let the loss function be $\mathbb{E}_x[(\sum_i u_i \sigma(w_i x) - y)^2/2]$, where $\sigma(x) = c_0 x + O(x^2)$ is any nonlinearity that is locally linear at $x = 0$. We let $c_0 = 1$ and focus on the case where both x and y are one-dimensional. Locally around $w \approx 0$, the model uw is either rank-1 or rank-0. The rank-0 point where $u_i = w_i = 0$ for all i is a saddle point as long as $\mathbb{E}[xy] \neq 0$. In this section, we show that the stability of this saddle point features complex and dramatic phase transition-like behaviors as we change the learning rate of SGD.

Consider the linearized dynamics around the saddle at $w = u = 0$. The expanded loss function takes the form:

$$\ell(u, w) = -xy \sum_i^d u_i w_i + \text{const.} \quad (11)$$

For learning to happen, SGD needs to escape from the saddle point. For analytical tractability, we let $xy = 1$ with probability 0.5 and $xy = a$; otherwise, for a controllable parameter a . When $a > -1$, *correct* learning happens when $\text{sign}(w) = \text{sign}(u)$. We thus focus on the case when $a > -1$. The case for $a < -1$ is symmetric to this case up to a rescaling. We solve the probabilistic stability regimes of this saddle in Section A.6. See Figure 1 (b). The two most important observations are: (1) SGD can indeed converge to low-rank saddle points; however, this happens only when the gradient noise is sufficiently strong and when the learning rate is large (but not too large); (2) the region for convergence to saddles (region III) is exclusive with the region for convergence in mean square (Ia), and thus one can only understand the saddle-seeking behavior of SGD within the proposed probabilistic framework. Rigorously, we prove the following proposition. It becomes evident that the low-rank solution is reached when both $w_t + u_t \rightarrow_p 0$ and $w_t - u_t \rightarrow_p 0$.

Proposition 2. *For any $w_0, u_0 \in \mathbb{R}/\{0\}$. $w_t - u_t \rightarrow_p 0$ if and only if $\mathbb{E}_x[\log|1 - \lambda xy|] < 0$. $w_t + u_t$ converges to 0 in probability if and only if $\mathbb{E}_x[\log|1 + \lambda xy|] < 0$.*

We present empirical demonstrations of this effect in Section 4.4. Many recent works have suggested how neural networks could be biased toward low-rank solutions. Theoretically, Galanti and Poggio (2022) showed that with a weak weight decay, SGD is biased towards low-rank solutions. Ziyin et al. (2022a) showed that with weight decay, GD converges to a low-rank solution. Therefore, weight decay already induces a low-rank bias in learning, and it is not known if SGD on its own has any bias toward low-rank solutions. Andriushchenko et al. (2022) showed empirical hints of a preference of low-rank solutions when training without SGD. However, it remains to be clarified when or why SGD has such a preference on its own. To the best of our knowledge, our theory is the first to precisely characterize the low-rank bias of SGD in a deep learning setting. Compared with the stability diagram of linear regression, this result implies that a large learning rate can both help and hinder optimization.

Our theory shows that the phase diagram of SGD is a function of the data distribution, and it is interesting to explore and compare a few different settings. We consider a size- N Gaussian data. Let $x_i \sim \mathcal{N}(0, 1)$ and noise $\epsilon_i \sim \mathcal{N}(0, 4)$, and generate a noisy label $y_i = \mu x_i + (1 - \mu)\epsilon_i$. See the phase diagram for this dataset in Figure 3 for an infinite N . The phase diagrams in Figure 4 show the phase diagram for a finite N . We see that the phase diagram has a very rich structure at a finite size. We make three rather surprising observations about the phase diagrams: (1) as $N \rightarrow \infty$, the phase diagram tends to be something smooth and quite universal; (2) phase II seems to disappear as N becomes large; (3) the lower part of the phase diagram seems universal, taking the same shape for all samplings of the datasets and across different sizes of the dataset. This suggests that the convergence to low-rank structures can be a universal aspect of SGD dynamics, which corroborates the widely observed phenomenon of collapse in deep learning (Papayan et al., 2020; Wang and Ziyin, 2022; Tian, 2022). The theory also shows that if we fix the learning rate and noise level, increasing the batch size makes it more and more difficult to converge to the low-rank solution (see section B). This is expected because the larger the batch size, the smaller the effective noise in the gradient.

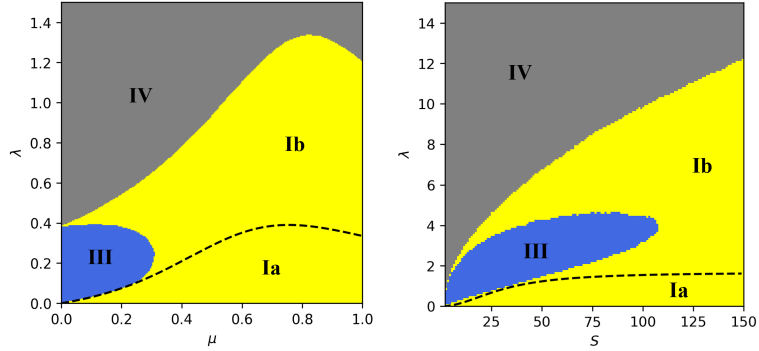


Figure 3: **Phase diagrams of SGD stability.** The definitions of the phases are the same as Figure 1. We sample a dataset of size N such that $x \sim \mathcal{N}(0, 1)$ and noise $\epsilon \sim \mathcal{N}(0, 4)$, and generate a noisy label $y = \mu x + (1 - \mu)\epsilon$. Left: the $\lambda - \mu$ phase diagram for $S = 1$ and $N = \infty$. Right: The $\lambda - S$ phase diagram for $\mu = 0.06$ and $N = \infty$.

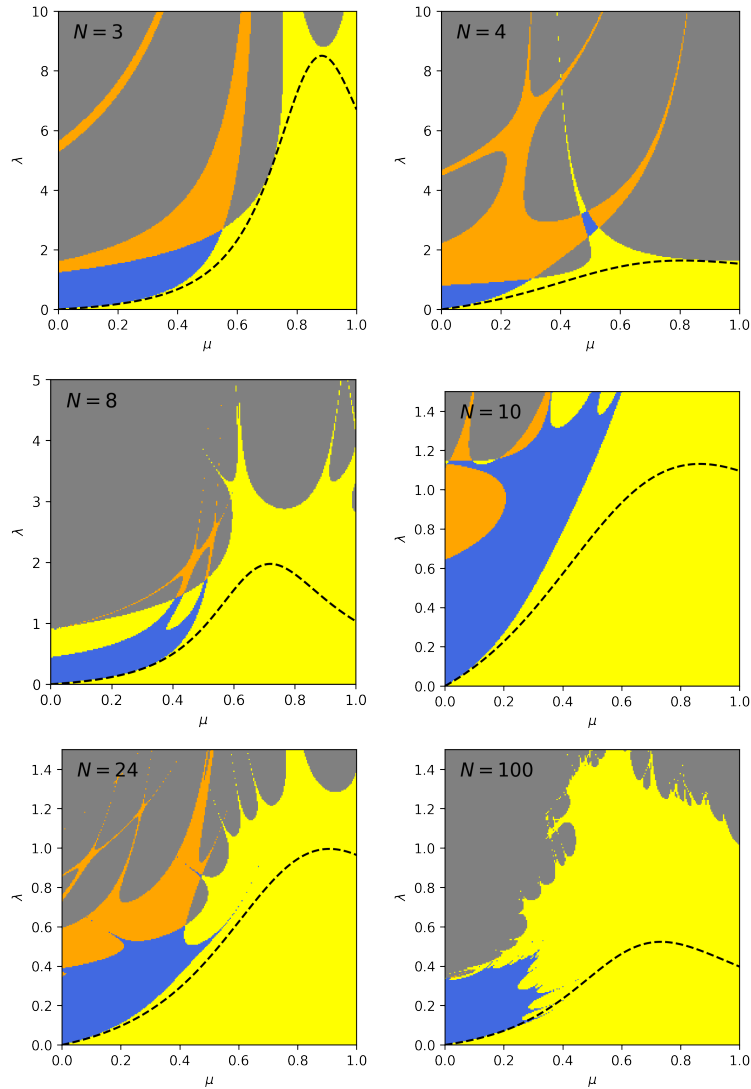


Figure 4: **Phase diagrams of SGD stability for finite-size dataset.** The sampling of the data is the same as in Figure 3. From upper left to lower right: $N = 3, 4, 8, 10, 24, 100$. As the dataset size tends to infinity, the phase diagram converges to that in Figure 3. The lower parts of all the phase diagrams look very similar, suggesting a universal structure.

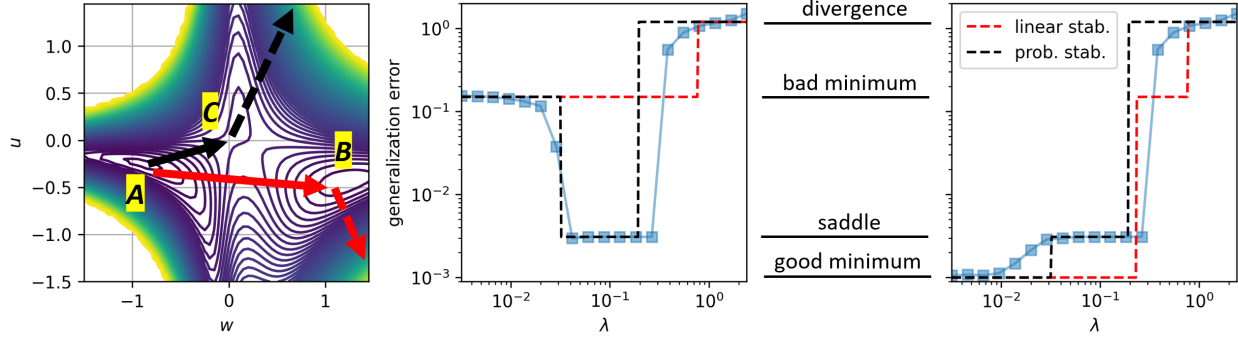


Figure 5: **How SGD selects a solution.** **Left:** The landscape of a two layer network with the swish activation function (Ramachandran et al., 2017). **Middle, Right:** the generalization performance of the model as one increases the learning rate. **Middle:** Initialized at solution B, SGD first jumps to C and then diverge. **Right:** Initialized at A, SGD also jumps to C and diverge. In both cases, the behavior of SGD agrees with the prediction of the probabilistic stability, instead of the linear stability. Instead of jumping between local minima, SGD at a large learning rate transitions from minima to saddles.

4.3 How SGD Selects a Solution

We now investigate one of the most fundamental problems in deep learning: how SGD selects a solution for a neural network. In this section, we study a two-layer network with a single hidden neuron with the swish activation function: $f(w, u, x) = u \times \text{swish}(wx)$, where $\text{swish}(x) = x \times \text{sigmoid}(x)$. Swish is a differentiable variant of ReLU that is discovered by meta-learning techniques and consistently outperforms ReLU in various tasks. We generate 100 data points (x, y) as $y = 0.1\text{swish}(x) + 0.9\epsilon$, where both x and ϵ are sampled from normal distributions. See Figure 5 for an illustration of the training loss landscape. Here, there are two local minima: solution A at roughly $(-0.7, -0.2)$ and solution B at $(1.1, -0.3)$. Here, the solution with better generalization is A because it captures the correct correlation between x and y when x is small. Solution A is also sharper; its largest Hessian eigenvalue is roughly $h_a = 7.7$. Solution B is the worse solution; it is also flatter, with the largest Hessian value being $h_b = 3.0$. There is also a saddle point C at $(0, 0)$, which performs significantly better than B and slightly worse than A in generalization.

If we initialize the model at A, linear stability theory would predict that as we increase the learning rate, the model moves from the sharper solution A to the flatter minimum B when SGD loses linear stability in A; the model would then lose total stability once SGD becomes linearly unstable at (b). As shown by the red arrows in Figure 5. In contrast, probabilistic stability predicts that SGD will move from A to C as C becomes attractive and then lose stability, as indicated by the black arrows. See the right panel of the figure for the comparison with the experiment for the model’s generalization performance. The dashed lines show the predictions of the linear stability theory and the probabilistic theory, respectively. We see the probabilistic theory predicts both the error and the place of transition right, whereas linear stability neither predicts the right transition nor the correct level of performance.

If we initialize at B, the flatter minimum, linear stability theory would predict that as we increase the learning rate, the model will only have one jump from B to divergence. Thus, from linear stability, SGD would have roughly the performance of B until it diverges, and having a large learning rate will not help with performance. In sharp contrast, the probabilistic stability predicts that the model will have two jumps: it stays at B for a small λ and jumps to C as it becomes attractive at an intermediate learning rate. The model will ultimately diverge if C loses stability. Thus, our theory predicts that the model will first have a bad performance, then a better performance at an intermediate learning rate, and finally diverge. See the middle panel of Figure 5. We see that the prediction of the probabilistic stability agrees with the experiment and correctly explains why SGD leads to a better performance of the neural network.

4.4 Neural Network Phase Diagrams

We start with a controlled experiment where, at every training step, we sample input $x \sim \mathcal{N}(0, I_{200})$ and noise $\epsilon \sim \mathcal{N}(0, 4I_{200})$, and generate a noisy label $y = \mu x + (1 - \mu)\epsilon$. Note that $1 - \mu$ controls the level of the

noise. Training proceeds with SGD on the MSE loss. We train a two-layer model with the architecture: $200 \rightarrow 200 \rightarrow 200$. See Figure 7 for the theoretical phase diagram. SGD escapes from the saddle with a finite variance to the right of the dashed line and has an infinite variance to its left. In the region $\lambda \in (0, 0.2)$, this loss of linear stability condition coincides with the condition for the convergence to the saddle. The experiment shows that the theoretical boundary agrees well with the numerical results. For completeness, we show that the Adam optimizer (Kingma and Ba, 2014) also has a qualitatively similar phase diagram in Appendix B. This suggests that the effects we studied in this work are rather universal, not just a special feature of SGD.

Lastly, we train independently initialized ResNets on CIFAR-10 with SGD. The training proceeds with SGD without momentum at a fixed learning rate and batch size $S = 32$ (unless specified otherwise) for 10^5 iterations. Our implementation of Resnet18 contains 11M parameters in total and achieves 94% test accuracy under the standard training protocol, consistent with the established values. To probe the effect of noise, we artificially inject a dynamical label noise during every training step, where, at every step, a correct label is flipped to a random label with probability *noise*. See Figure 1. We see that the results agree with the theoretical expectation and with the phase diagram of simpler models. We also study the sparsity of the ResNets in different layers in Appendix B, and we observe that the phase diagrams are all qualitatively similar. We also note that the effect is not due to having a dynamical label noise. Our experiments with a static label noise also show the same results with almost the same regime boundaries.

5 Discussion

In this work, we have demonstrated that the convergence in probability condition serves as an essential notion for understanding the stability of SGD, leading to highly nontrivial and practically relevant phase diagrams at a finite learning rate. We also clarified its connection to Lyapunov exponents, which are conventional and easy-to-measure metrics of stability in the study of dynamical systems. At a small learning rate and large batch size, the proposed stability agrees with the conventional notion of stability. At a large learning rate and a small batch size, we have shown that the proposed notion of stability captures the actual behavior of SGD much better and successfully explained a series of experiment phenomena that had been quite puzzling. Among the many implications that we discussed, perhaps the most fundamental one is a novel understanding of the implicit bias of SGD. When viewed from a dynamical stability point of view, the implicit bias of stochastic gradient descent is thus fundamentally different from the implicit bias of gradient descent. The new perspective we provide is also different from the popular perspective that SGD influences the learning outcome directly by making the model converge to flat minima. In fact, in our construction, the flatter minimum does not have better generalization properties, nor does SGD favor it over the sharper one. Instead, SGD performs a selection between converging to saddles and local minima, which directly and significantly affects its performance. Thus, we believe that the probabilistic stability is an important future direction to investigate the stability of SGD in a deep learning scenario through this new angle we suggested.

In the current work, our analysis centers around studying when and why the quantity $m := \mathbb{E}[\log |w_t - w^*|]$ becomes positive and does not discuss too much what the magnitude of m means. In fact, the quantity m tells us that the quantity $|w_t - w^*|$ is typically evolving like

$$|w_t - w^*| \propto e^m, \tag{12}$$

and, therefore, m can be seen as a robust metric of the convergence rate of the system. Thus, m/t can be seen as a metric of the time scale of the relevant dynamics in the neighborhood of a stationary point. Moreover, it is much more informative than the common metric of convergence in the theoretical literature, such as the expected regret or the training loss. As we have argued, these quantities are not good metrics of convergence because they are dominated by rare outliers of trajectories and can diverge even if the system is probabilistically stable. What makes the problem worse is the fact that at a large learning rate, such outlier trajectories lead to divergence of fluctuation. In this sense, m reflects the *typical* behavior of training much better. See Section B.1, where we compare e^{2m} with sample trajectories of learning empirically.

Practitioners often plot the training loss in a logarithmic scale vs. training iteration to monitor the progress, where the training loss is estimated by a minibatch sampling. For example, see Figure 2 and 3 of (Kingma and Ba, 2014). Looking at the logarithmic scale often gives us a much better grasp of how the

training is progressing than looking at the raw training loss. This is essentially monitoring the quantity m_L . Our theory, thus, offers a first step towards understanding a more practically relevant metric of training progress.

References

- Andriushchenko, M., Varre, A., Pillaud-Vivien, L., and Flammarion, N. (2022). Sgd with large step sizes learns sparse features. *arXiv preprint arXiv:2210.05337*.
- Brea, J., Simsek, B., Illing, B., and Gerstner, W. (2019). Weight-space symmetry in deep networks gives rise to permutation saddles, connected by equal-loss valleys across the loss landscape. *arXiv preprint arXiv:1907.02911*.
- Eckmann, J.-P. and Ruelle, D. (1985). Ergodic theory of chaos and strange attractors. *The theory of chaotic attractors*, pages 273–312.
- Galanti, T. and Poggio, T. (2022). Sgd noise and implicit low-rank bias in deep neural networks. *arXiv preprint arXiv:2206.05794*.
- Ge, R., Lee, J. D., and Ma, T. (2016). Matrix completion has no spurious local minimum. *Advances in neural information processing systems*, 29.
- Gower, R. M., Loizou, N., Qian, X., Sailanbayev, A., Shulgin, E., and Richtárik, P. (2019). Sgd: General analysis and improved rates. In *International conference on machine learning*, pages 5200–5209. PMLR.
- He, F., Liu, T., and Tao, D. (2019). Control batch size and learning rate to generalize well: Theoretical and empirical evidence. *Advances in Neural Information Processing Systems*, 32.
- Hoffer, E., Hubara, I., and Soudry, D. (2017). Train longer, generalize better: closing the generalization gap in large batch training of neural networks. In *Advances in Neural Information Processing Systems*, pages 1731–1741.
- Kawaguchi, K. (2016). Deep learning without poor local minima. *Advances in Neural Information Processing Systems*, 29:586–594.
- Kingma, D. P. and Ba, J. (2014). Adam: A method for stochastic optimization. *CoRR*, abs/1412.6980.
- Li, Y., Wei, C., and Ma, T. (2019). Towards explaining the regularization effect of initial large learning rate in training neural networks. *Advances in Neural Information Processing Systems*, 32.
- Liu, K., Ziyin, L., and Ueda, M. (2021). Noise and fluctuation of finite learning rate stochastic gradient descent.
- Liu, Y., Gao, Y., and Yin, W. (2020). An improved analysis of stochastic gradient descent with momentum. *Advances in Neural Information Processing Systems*, 33:18261–18271.
- Lu, H. and Kawaguchi, K. (2017). Depth creates no bad local minima. *arXiv preprint arXiv:1702.08580*.
- Lyapunov, A. M. (1992). The general problem of the stability of motion. *International journal of control*, 55(3):531–534.
- Mori, T., Ziyin, L., Liu, K., and Ueda, M. (2022). Power-law escape rate of sgd.
- Papayan, V., Han, X., and Donoho, D. L. (2020). Prevalence of neural collapse during the terminal phase of deep learning training. *Proceedings of the National Academy of Sciences*, 117(40):24652–24663.
- Ramachandran, P., Zoph, B., and Le, Q. V. (2017). Searching for activation functions.
- Shirish Keskar, N., Mudigere, D., Nocedal, J., Smelyanskiy, M., and Tang, P. T. P. (2016). On Large-Batch Training for Deep Learning: Generalization Gap and Sharp Minima. *ArXiv e-prints*.

- Tian, Y. (2022). Deep contrastive learning is provably (almost) principal component analysis. *arXiv preprint arXiv:2201.12680*.
- Vaswani, S., Bach, F., and Schmidt, M. (2019). Fast and faster convergence of sgd for over-parameterized models and an accelerated perceptron. In *The 22nd international conference on artificial intelligence and statistics*, pages 1195–1204. PMLR.
- Wang, Z. and Ziyin, L. (2022). Posterior collapse of a linear latent variable model. *arXiv preprint arXiv:2205.04009*.
- Wu, L., Ma, C., et al. (2018). How sgd selects the global minima in over-parameterized learning: A dynamical stability perspective. *Advances in Neural Information Processing Systems*, 31.
- Wu, L., Wang, M., and Su, W. (2022). When does sgd favor flat minima? a quantitative characterization via linear stability. *arXiv preprint arXiv:2207.02628*.
- Xie, Z., Sato, I., and Sugiyama, M. (2020). A diffusion theory for deep learning dynamics: Stochastic gradient descent exponentially favors flat minima. *arXiv preprint arXiv:2002.03495*.
- Zhu, Z., Wu, J., Yu, B., Wu, L., and Ma, J. (2018). The anisotropic noise in stochastic gradient descent: Its behavior of escaping from sharp minima and regularization effects. *arXiv preprint arXiv:1803.00195*.
- Ziyin, L., Li, B., and Meng, X. (2022a). Exact solutions of a deep linear network. *arXiv preprint arXiv:2202.04777*.
- Ziyin, L., Liu, K., Mori, T., and Ueda, M. (2022b). Strength of minibatch noise in SGD. In *International Conference on Learning Representations*.

A Additional Theoretical Concerns

A.1 Convergence at a special learning rate

Proposition 3. Consider a dataset where all the data points $(x_i, y_i) \in \mathbb{R}^2$ lie on a straight line. For any initialization, w_0 and learning rate $\lambda = 1/x_i^2$, stochastic gradient descent (SGD) converges to the global minimum $w^* = x_i/y_i$ with probability 1.

Proof. Let us examine a single step of SGD dynamics. With probability $1/N$, the algorithm selects data point x_i for training, and the update rule is as follows:

$$w_{t+1} = w_t - \lambda x_i(x_i w_t - y_i) = y_i/x_i. \quad (13)$$

Thus, we can update w_t to $w_{t+1} = y_i/x_i$ with probability $\geq 1/N$. Once w_t reaches the global minimum y_i/x_i , it stays there with zero probability of leaving because it is the unique minimum. Hence, for any initialization w_0 , we have

$$\mathbb{P}(w_t \neq y_i/x_i) \leq (1 - \frac{1}{N})^t \rightarrow 0. \quad (14)$$

This concludes the proof. \square

A.2 Linear Stability Conditions and the Derivation of Eq. (4)

A.2.1 General Condition for Dynamical Stability

For a general batch size S , the dynamics of SGD reads

$$w_{t+1} = w_t - \lambda w_t \frac{1}{S} \sum_{i=1}^S x_i^2 \quad (15)$$

$$= w_t \left(1 - \lambda \frac{1}{S} \sum_{i=1}^S x_i^2 \right). \quad (16)$$

The second moment of w_{t+1} is

$$\mathbb{E}_x[w_{t+1}^2 | w_t] = w_t^2 \mathbb{E}_x \left(1 - \lambda \frac{1}{S} \sum_i x_i^2 \right)^2 \quad (17)$$

$$= w_t^2 \left(1 - 2\lambda \mathbb{E}[x^2] + \frac{\lambda^2}{S^2} \sum_{i,j} \mathbb{E}[x_i^2 x_j^2] \right) \quad (18)$$

$$= w_t^2 \left(1 - 2\lambda \mathbb{E}[x^2] + \frac{\lambda^2}{S^2} \mathbb{E}[x^4] + \frac{\lambda^2 (S-1)^2}{S^2} \mathbb{E}[x^2]^2 \right). \quad (19)$$

Note that this equation applies to any $w_t \in \mathbb{R}$. Therefore, the second moment of w_t is convergent if

$$\left(1 - 2\lambda \mathbb{E}[x^2] + \frac{\lambda^2}{S^2} \mathbb{E}[x^4] + \frac{\lambda^2 (S-1)^2}{S^2} \mathbb{E}[x^2]^2 \right) < 1, \quad (20)$$

which solves to

$$\lambda < \frac{2S^2 \mathbb{E}[x^2]}{\mathbb{E}[x^4] + (S-1)^2 \mathbb{E}[x^2]^2}. \quad (21)$$

This condition applies to any data distribution. One immediate observation is that it only depends on the second and fourth moments of the data distribution and that both moments need to be finite for convergence at a non-zero learning rate. It is quite instructive to solve this condition under a few special conditions.

A.2.2 Gaussian Data Distribution

The condition (21) takes a precise form when the data is Gaussian. Using the fact that for a Gaussian variable x with variance σ^2 , $\mathbb{E}[x^4] = 3\sigma^4$, the condition simplifies to

$$\lambda < \frac{2}{\mathbb{E}[x^2]} \frac{S^2}{3S + (S-1)^2}. \quad (22)$$

This is the same as Eq. (4).

A.2.3 Bernoulli Dataset

Another instructive case to consider is the case when there are only two data points in the data: x_1 and x_2 . The moments are

$$\begin{cases} \mathbb{E}[x^2] = \frac{1}{2}(x_1^2 + x_2^2), \\ \mathbb{E}[x^4] = \frac{1}{2}(x_1^4 + x_2^4). \end{cases} \quad (23)$$

When one of the data points, say x_1 , is very large, the condition becomes

$$\lambda < \frac{2S^2 x_1^2}{2x_1^4 + (S-1)^2 x_1^4} = \frac{2S^2}{x_1^2} \frac{1}{2 + (S-1)^2}. \quad (24)$$

A.2.4 Extreme Outlier

We can also consider the general case of a finite dataset with a large outlier, x_{\max} . The condition is similar to the Bernoulli case. We have

$$\begin{cases} \mathbb{E}[x^2] \approx \frac{1}{N} x_{\max}^2, \\ \mathbb{E}[x^4] \approx \frac{1}{N} x_{\max}^4. \end{cases} \quad (25)$$

The condition reduces to

$$\lambda < \frac{2S^2}{N x_{\max}^2} \frac{1}{1 + \frac{(S-1)^2}{N}}. \quad (26)$$

This can be seen as the generalization of the Bernoulli condition. When $S = 1$, this condition becomes

$$\lambda < \frac{2}{N x_{\max}^2}. \quad (27)$$

There are many other interesting limits of this condition we can consider from the perspective of extreme value theory. However, this is beyond the scope of this work and we leave it as an interesting future work.

A.3 Non-interpolating case

In this section, we show that consistent with our previous theory, the convergence to a stationary distribution is possible for learning rates far larger than a linear stability theory would expect. We only discuss the main steps and conclusions in the main text. The formal analysis is left to the appendix. To keep the computation concise, we focus on the case when the learning rates are ‘‘critical’’. Namely, we let $\lambda = 1/x_i^2$ for some i . Here, the SGD dynamics implies

$$|w_{t+1}| = \begin{cases} |y_i/x_i| & \text{with probability } 1/N; \\ |a_t w_t + b_t| & \text{otherwise,} \end{cases} \quad (28)$$

where a and b are constants depending on the batch at step t . Such a dynamics is upper bounded by an alternative dynamics that is independent of the other data points:

$$|z_{t+1}| = \begin{cases} |y_i/x_i| & \text{with probability } 1/N; \\ |a|z_t + |b| & \text{otherwise,} \end{cases} \quad (29)$$

where $a = \max_t |a_t|$, $b = \max_t |b_t|$, and $z_0 = w_0$. This dynamics is easy to study – its possible achievable values are discrete in space:

$$|y_i/x_i| a^j + b a^j \frac{1 - (1/a)^j}{1 - 1/a} \approx a^j \left(|y_i/x_i| + \frac{ab}{a-1} \right) \quad (30)$$

for all $j \in \mathbb{Z}^+$. The number j is thus a natural index for indexing these states. One can show that in the infinite time limit, any bounded starting distribution converges to a unique stationary distribution:

$$\mathbb{P} \left(z_j = |y_i/x_i| a^j + b a^j \frac{1 - (1/a)^j}{1 - 1/a} \right) = \frac{1}{N} (1 - 1/N)^j, \quad (31)$$

which upper bounds the distribution of w . Therefore, w does not diverge as long as z does not diverge. One interesting question is how likely is w to be away from y_i/x_i . Let $\epsilon_j = a^j (|y_i/x_i| + \frac{ab}{a-1})$. We have

$$\mathbb{P}(z \geq \epsilon_j) = \mathbb{P}(z = \epsilon_j) + \mathbb{P}(z = \epsilon_{j+1}) + \dots \quad (32)$$

$$= \sum_{k=j}^{\infty} \frac{1}{N} (1 - 1/N)^k \quad (33)$$

$$= (1 - 1/N)^j \quad (34)$$

$$\propto \epsilon_j^{-\frac{1}{N \log a}} \quad (35)$$

This result means that the distribution of the parameter w has a power-law tail. The exponent decides the thickness of this tail. The closer the exponent to zero, the less likely the parameter will be around the minimum. Here, we see that the scaling exponent is proportional to the growth factor $\log a$, where

$$\log a = \log |1 - \lambda h|. \quad (36)$$

In the worst case scenario, $h = x_{\max}^2$. However, in the average case, one expects h to be close to the average data norm: $h \approx \mathbb{E}_x[x^2]$. Thus, when the learning rate is not too large, we have that the exponent is $\propto \frac{1}{\lambda \mathbb{E}[x^2]}$. When λ is very large, the scaling exponent becomes logarithmic: $1/\log(\lambda \mathbb{E}[x^2])$. In both cases, the scaling is clear: the large the learning rate, the heavier the tail of the distribution. This is consistent with the previous results [Mori et al. \(2022\)](#). While one often interprets this power-law behaviors as that SGD encourages exploration, we interpret this conversely – the model parameter has a significant nonzero probability of staying around the given local minimum. In practice, it is very likely such local minimum are reflected in a robust estimator of the parameter.

A.4 Proofs

A.4.1 Proof of Proposition 1

Proof. First of all, when $\lambda = 1/x_i^2$, the convergence is almost sure, which implies convergence in probability. Thus, we focus on the case when $\lambda = 1/x_i^2 \neq 0$ for all i . Note that this condition is equivalent to that $\mathbb{E}_x[1 - \lambda x^2]$ is not infinite.

Now, the dynamics Eq. (6) implies the following dynamics

$$w_{t+1}/w_t = 1 - \lambda x_t^2, \quad (37)$$

which implies

$$|w_{t+1}/w_0| = \prod_{\tau=1}^t |1 - \lambda x_\tau^2|. \quad (38)$$

We can define auxiliary variables $z_t := \log |w_{t+1}/w_0| - m$ and $m := \mathbb{E} \log |w_{t+1}/w_0| = t \mathbb{E}_x \log |1 - \lambda x^2|$. Also define $s := \text{Var}[\log |1 - \lambda x^2|]$. Let $\epsilon > 0$. We have that

$$\mathbb{P}(|w_t| < \epsilon) = \mathbb{P}(|w_0| e^{z_t + m} < \epsilon) \quad (39)$$

$$= \mathbb{P}\left(\frac{1}{t} z_t < \frac{1}{t} (\log \epsilon / |w_0| - m)\right) \quad (40)$$

$$= \mathbb{P}(z_t/t < -\mathbb{E}_x \log |1 - \lambda x^2| + o(1)) \quad (41)$$

By the law of large numbers, the left-hand side of the inequality converges to 0, whereas the right-hand side converges to a constant. Thus, we have, for all $\epsilon > 0$,

$$\lim_{t \rightarrow \infty} \mathbb{P}(|w_t| < \epsilon) = \begin{cases} 1 & \text{if } m < 0 \\ 0 & \text{if } m > 1. \end{cases} \quad (42)$$

This completes the proof. \square

A.4.2 Proof of Theorem 1

Proof. First of all, we define $z_t = \hat{m}_g(w_t) - m_g(t)$. By definition, we have

$$\mathbb{P}(\|\Delta g_t\| < \epsilon) = \mathbb{P}(e^{z_t + m_g(t)} < \epsilon) \quad (43)$$

$$= \mathbb{P}\left(\frac{1}{t}z_t < \frac{1}{t}(\log \epsilon / |w_0| - m_w(t))\right) \quad (44)$$

$$= \mathbb{P}\left(\frac{1}{t}z_t < \frac{1}{t}m_w(t) + o(1)\right). \quad (45)$$

Now, because $\text{Var}[z_t] = \text{Var}[\log \|\Delta g(t)\|] = o(t^2)$, we have that $\text{Var}[z_t/t] = o(1)$. Applying Chebychev's inequality, one obtains that for any $\eta > 0$

$$\mathbb{P}(z_t/t > \eta) \leq \frac{\text{Var}[z_t/t]}{\eta^2} \rightarrow 0. \quad (46)$$

This means that z_t/t converges to 0 in mean square. In turn, this implies that

$$\lim_{t \rightarrow \infty} \mathbb{P}(\|\Delta g_t\| < \epsilon) = \lim_{t \rightarrow \infty} \mathbb{P}\left(\frac{1}{t}z_t < \frac{1}{t}m_w(t)\right) = \begin{cases} 1 & \text{if } m < 0 \\ 0 & \text{if } m > 0. \end{cases} \quad (47)$$

This finishes the proof. \square

A.5 Convergence of Generic SGD Dynamics

In this section, we show that a generic SGD dynamics in multi-dimension obeys Proposition 1. Recall that the dynamics of SGD close to a *non-fluctuating* stationary point is

$$w_{t+1} - w^* = w_t - \frac{2\lambda}{S} \sum_{j=1}^S \hat{H}(w^*, x_j)(w_t - w^*), \quad (48)$$

where $\hat{H}(w, x) := \nabla_w^2 \ell(w, x)$ is the sample-wise Hessian. Note that we allow H to have negative eigenvalues so that our result includes the case where w^* is a saddle point. It suffices to prove for the case $S = 1$ and N is finite.

Theorem 2. *Let w_t obey Eq. (48), and $\hat{m}_t = \log \|w_t - w^*\|$. Let $I - \lambda \hat{H}_i$ be full rank for all i . Then,*

$$\lim_{t \rightarrow 0} \text{Var}[\hat{m}_t/t] = 0. \quad (49)$$

Proof. Without loss of generality, we let $w^* = 0$. By assumption, $\lim_{t \rightarrow \infty} \hat{m}_t/t = c_0 \neq 0$. By definition, we have that

$$\text{Var}[\hat{m}_t/t] = \frac{1}{t^2} (\mathbb{E}[\hat{m}_t^2] - m_t^2). \quad (50)$$

We thus need to compute $\mathbb{E}[\hat{m}_t^2]$.

By assumption, $I - \lambda \hat{H}_i$ is full rank, we can thus define r_{\max} to be larger than the absolute value of all the eigenvalues of $I - \lambda \hat{H}_i$ for all i . Similarly, we can define $r_{\min} > 0$ to be smaller than all the absolute values of all the eigenvalues of $I - \lambda \hat{H}_i$ for all i . Note that by definition, $r_{\min} < e^{c_0} < r_{\max}$, and so we can choose r_{\min} and r_{\max} such that

$$\frac{1}{2}(\log r_{\min} + \log r_{\max}) = m. \quad (51)$$

Now, we use r_{\min} and r_{\max} to construct an auxiliary process that upper bounds the variance of \hat{m}_t . Let

$$\mu_{t+1} = \mu_t + \log r, \quad (52)$$

where $r = r_{\min}$ with probability 0.5, and $r = r_{\max}$ with probability 0.5. Note that by definition,

$$\mathbb{E}[\mu_t/t] = c_0, \quad (53)$$

and

$$\text{Var}[\mu_t/t] = \frac{1}{2t} [(\log r_{\max} - c_0)^2 + (\log r_{\min} - c_0)^2] = O(t^{-1}). \quad (54)$$

However, for any fixed w_t , we have that

$$\|w_{t+1}\| = \|(I - \lambda \hat{H}_{i_t})w_t\|, \quad (55)$$

which implies that

$$r_{\min}\|w_t\| \leq \|w_{t+1}\| \leq r_{\max}\|w_t\|. \quad (56)$$

which implies that

$$\text{Var}[\hat{m}_{t+1}|\hat{m}_t] \leq \text{Var}[\mu_{t+1}|\mu_t]. \quad (57)$$

In turn, this implies that if $\mu_0 = \hat{m}_0$

$$\text{Var}[\hat{m}_t/t] \leq \text{Var}[\mu_t/t] \quad (58)$$

for all t . Taking the infinite time limit on both sides, we have that

$$\text{Var}[\hat{m}_t/t] \rightarrow 0. \quad (59)$$

The proof is complete. \square

Therefore, SGD dynamics satisfies the assumption of Proposition 1. Another important question is whether this theorem is trivial for SGD at a high dimension in the sense that it could be the case that m_t could be identically zero independent of the dataset. One can show that for all datasets that satisfy a very mild condition, the Lyapunov exponent is, in general, nonzero.

Let $\mathbb{E}[\hat{H}]$ be full rank. Let \hat{m}_t be defined as in the previous proof. By definition,

$$\mathbb{E}[\hat{m}_t] = \mathbb{E}[\log w_0^T \left(\prod_j^t (I - \lambda \hat{H}_{i_j}) \right) \left(\prod_j^t (I - \lambda \hat{H}_{i_j}) \right)^T w_0]. \quad (60)$$

Again, let $w^* = 0$. When λ is small, this can be expanded as

$$\mathbb{E}[m_t] = \mathbb{E} \log \left(\|w_0\|^2 + 2\lambda w_0^T \sum_j^t \hat{H}_j w_0 + O(\lambda^2) \right) \quad (61)$$

$$= \log \|w_0\|^2 + \frac{\mathbb{E}[2\lambda w_0^T \sum_j^t \hat{H}_j w_0]}{\|w_0\|^2} + O(\lambda^2) \quad (62)$$

$$= \log \|w_0\|^2 + \frac{2\lambda t w_0^T H w_0}{\|w_0\|^2} + O(\lambda^2). \quad (63)$$

Therefore,

$$\lim_{t \rightarrow \infty} \mathbb{E}[\hat{m}_t/t] = -\frac{2\lambda w_0^T H w_0}{\|w_0\|^2} + O(\lambda^2). \quad (64)$$

Therefore, as long as λ is sufficiently small, the Lyapunov exponent is always negative. This proves something quite general for SGD at an interpolation minimum: with a small learning rate, the model converges to the minimum exponentially.

A.6 Proof of Proposition 2

Proof. To repeat, we consider the dynamics of SGD around a saddle:

$$\ell = -\chi \sum_i u_i w_i, \quad (65)$$

where we have combined xy into a single variable χ . The dynamics of SGD is

$$\begin{cases} w_{i,t+1} = w_{i,t} + \lambda \chi u_{i,t}, \\ u_{i,t+1} = u_{i,t} + \lambda \chi w_{i,t}. \end{cases} \quad (66)$$

Namely, we obtain a coupled set of stochastic difference equations. Since the dynamics is the same for all index i , we omit i from now on. This dynamics can be decoupled if we consider two transformed parameters: $h_t = w_t + u_t$, and $m_t = w_t - u_t$. The dynamics for these two variables is

$$\begin{cases} h_{t+1} = h_t + \lambda\chi h_t, \\ m_{t+1} = m_t - \lambda\chi m_t. \end{cases} \quad (67)$$

We have thus obtained two decoupled linear dynamics that take the same form as the linear regression problem we studied and our results on linear regression directly carry over. For example, as immediate corollaries, we know that h converges to 0 if and only if $\mathbb{E}[\log|1 + \lambda\chi|] < 0$, and m converges to 0 if and only if $\mathbb{E}[\log|1 - \lambda\chi|] < 0$.

When both h and m converge to zero in probability, we have that both w and u converge to zero in probability. For the data distribution under consideration, we have

$$\mathbb{E}[\log|1 + \lambda\chi|] = \frac{1}{2} \log|(1 + \lambda)(1 + \lambda a)| \quad (68)$$

and

$$\mathbb{E}[\log|1 - \lambda\chi|] = \frac{1}{2} \log|(1 - \lambda)(1 - \lambda a)|. \quad (69)$$

There are four cases: (1) both conditions are satisfied; (2) one of the two is satisfied; (3) none is satisfied. These correspond to four different phases of SGD around this saddle. \square

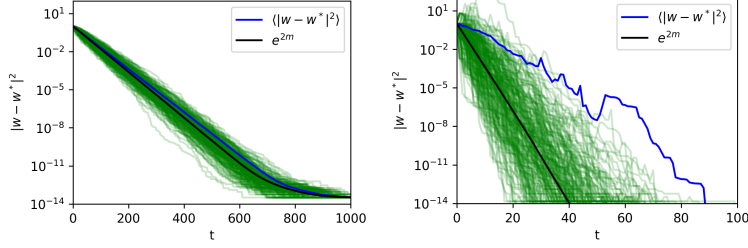


Figure 6: Dynamics and convergence rate of SGD as measured by the logarithmic rate (e^{2m}), and the squared error ($\langle |w_t - w^*|^2 \rangle$). The green lines show 200 independent samples of training. For a small learning rate (**left**), the two trajectories are similar, both agreeing quite well with the majority trajectories. For a large learning rate (**middle**), the proposed quantity e^{2m} agrees with the majority of the trajectories, whereas $\langle |w_t - w^*|^2 \rangle$ is dominated by rare trajectories that have lost stability, and is thus far larger than the typical trajectories. e^{2m} thus better reflects the convergence rate of the typical trajectories and is easy to estimate.

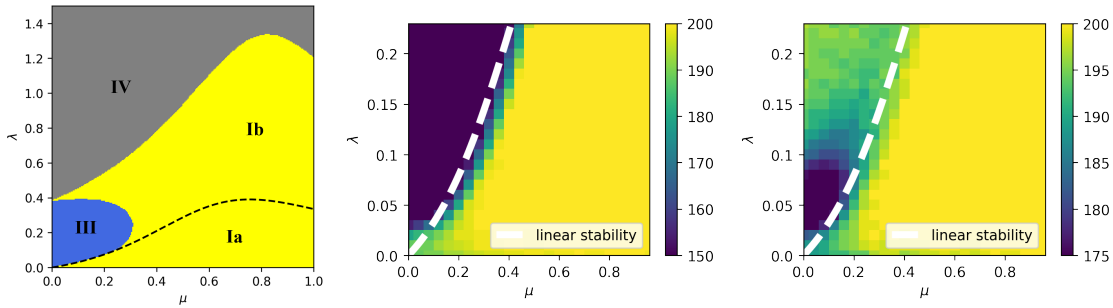


Figure 7: Convergence to low-rank solutions in nonlinear neural networks. At every training step, we sample input $x \sim \mathcal{N}(0, I_{200})$ and noise $\epsilon \sim \mathcal{N}(0, \sqrt{2}I_{200})$, and generate a noisy label $y = \mu x + (1 - \mu)\epsilon$. $1 - \mu$ controls the level of the noise. Left: the stability of the saddle low-rank saddle for a corresponding $1d$ input given by Proposition 1. We compare the rank of the last layer of a trained two-layer model for $\lambda \in (0, 0.25]$ with the theoretical prediction. Yellow region denotes full rank. The darker the color, the lower the rank of the trained model. **Middle**: Linear network. **Right**: tanh network. The red dashed line shows the theoretical prediction of the appearance of low-rank structure computed by numerically integrating the condition in Proposition 1.

B Additional Experiments

B.1 Typical training trajectories

See Figure 6. We see that e^{2m} better reflects the convergence rate of the typical trajectories and is easy to estimate. In contrast, the variance of SGD is very difficult to estimate and is dominated by outlier trajectories.

B.2 Neural Network Experiments

See Figure 7 presents the enlarged numerical results described in Section 4.4.

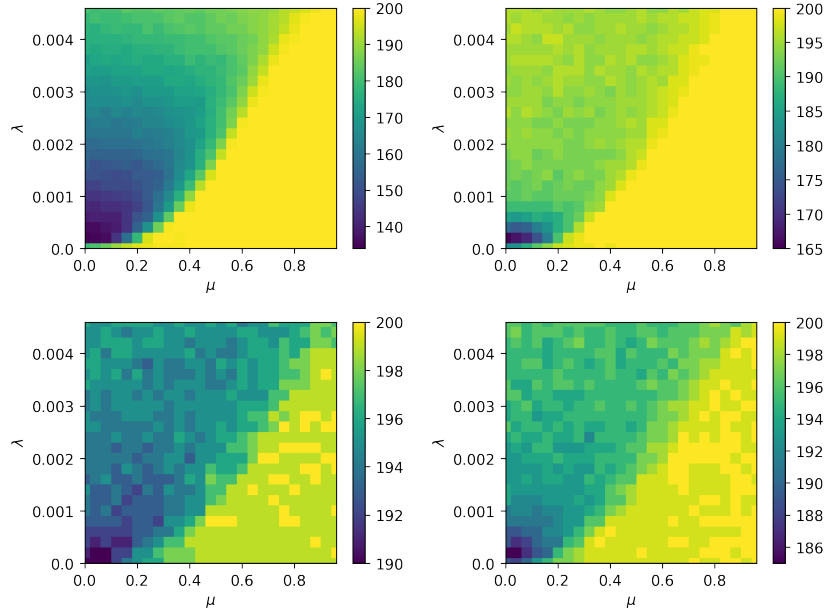


Figure 8: Rank of the converged solution for two-layer linear (upper left), tanh (upper right), relu (lower left) and swish (lower right) models.

B.3 Experiment with Adam

We note that the phenomena we studied is not just a special feature of the SGD, but, empirically, seems to be a universal feature of first-order optimization methods that rely on minibatch sampling. Here, we repeat the experiment in Figure 1. We train with the same data and training procedure, except that we replace SGD with Adam (Kingma and Ba, 2014), the most popular first-order optimization method in deep learning. Figure 8 shows that similar to SGD, Adam also converges to the low-rank saddles in similar regions of learning rate and μ .

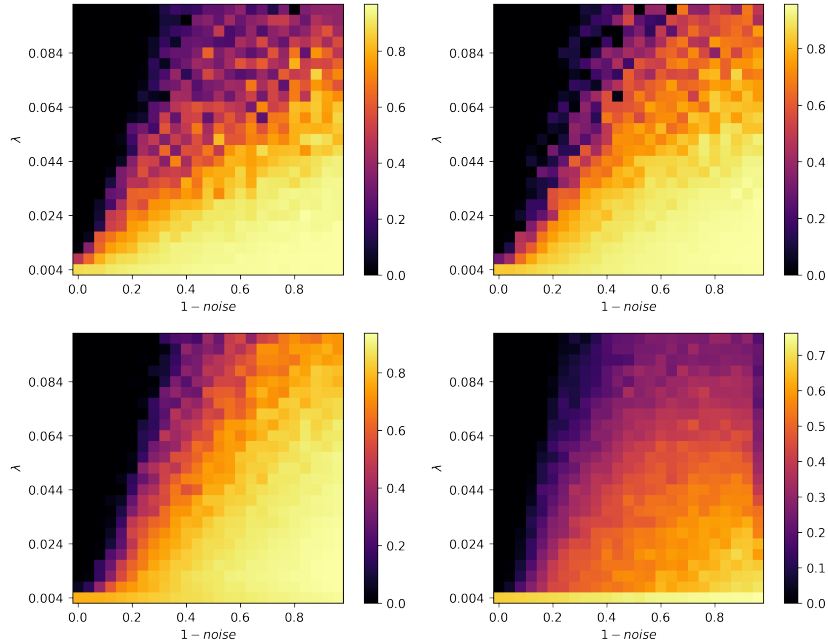


Figure 9: Sparsity of the convolutional layers in a ResNet18. Here, we show the number of parameters are approximately zero in the two of the largest convolutional layers, each containing roughly 1M parameters in total. The figure respectively show layer1.1.conv2 (upper left), layer2.1.conv2 (upper right), layer3.1.conv2 (lower left), layer4.1.conv2 (lower right).

B.4 ResNet18 Experiments

The task we study is the classification in CIFAR-10 using the ResNet18 model. The model is trained by SGD with a constant learning rate using a batch size of 32 for 10^5 iterations. The input images are augmented by random crops and random horizontal flips to reduce overfitting. Two hyperparameters, that is, learning rate and noise rate, are controlled during the experiments. The learning rate is defined conventionally, while the noise rate is the probability of reselecting the label from a uniform distribution for every input image at every iteration of training. The noise for each image is independent and is injected during training, so it adds uncertainty to the training and does not introduce bias to the data.

The trained model is evaluated by its accuracy on the test data set, sparsity of parameters, and the rank of the feature space. The sparsity of parameters is defined as the fraction of zero parameters in a specific layer. Before the last linear layer, our implementation of ResNet18 has 512 output nodes, which are also perceived as the 512 features encoded from the image. We randomly select 1000 images from the test data set of CIFAR-10 and calculate the 512 features for each of them, then find the dimensionality of the linear space of the 1000 512-dimensional vectors. See Figure 9.

Also, see Figure 12. The rank of the learned representation decreases as we decrease the batch size of SGD.

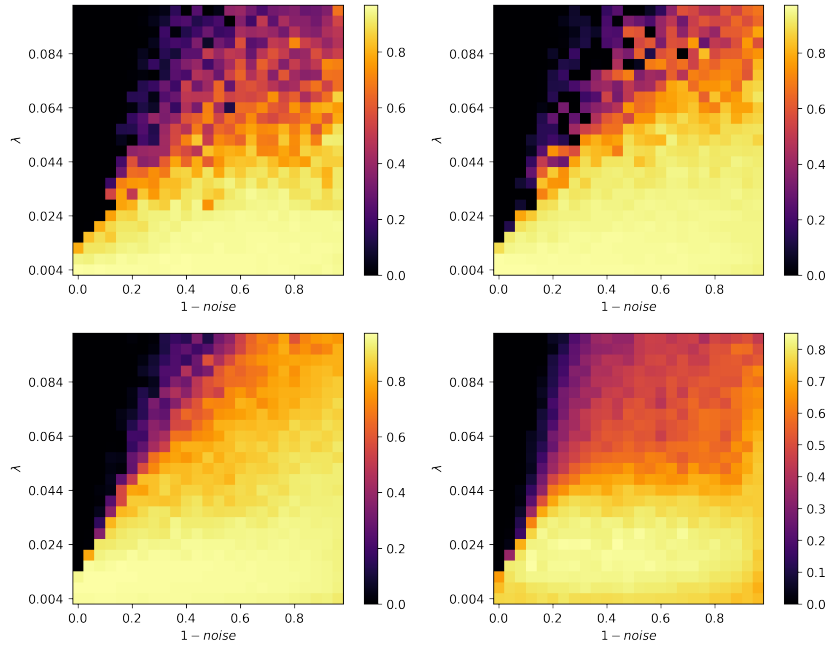


Figure 10: Sparsity of the convolutional layers in a ResNet18, when there is static noise in the training data. Here, we show the number of sparse parameters in the two of the largest convolutional layers, each containing roughly 1M parameters in total. The figures respectively show layer1.1.conv2 (upper left), layer2.1.conv2 (upper right), layer3.1.conv2 (lower left), and layer4.1.conv2 (lower right).

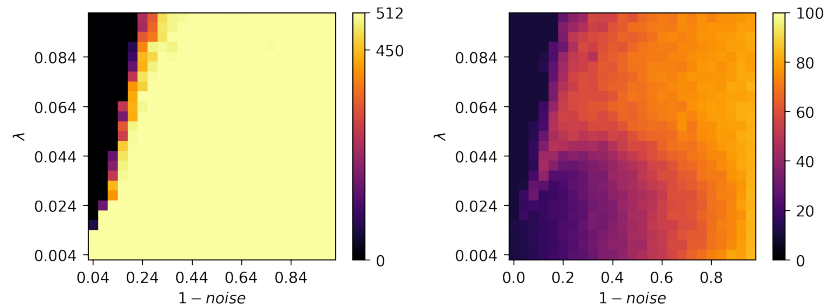


Figure 11: Rank (left) and test accuracy of the ResNet18 trained in a data set with static noise. The transition of the rank has a clear boundary. The model has full rank but random-guess level performance for large noise and small learning rates.

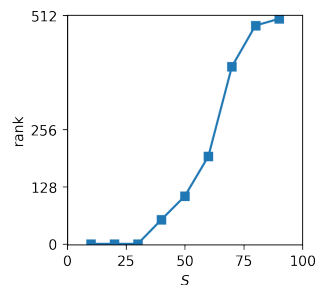


Figure 12: The rank of the penultimate-layer representation of Resnet18 trained with different levels of batch sizes. In agreement with the phase diagram, the model escapes from the low-rank saddle as one increases the batch size.